



# Discovery of a C-S lyase inhibitor for the prevention of human body malodor formation: tannic acid inhibits the thioalcohol production in *Staphylococcus hominis*

Ozkan Fidan<sup>1</sup> · Ayse Doga Karipcin<sup>2</sup> · Ayse Hamide Köse<sup>2</sup> · Ayse Anaz<sup>2</sup> · Beyza Nur Demirsoy<sup>2</sup> · Nuriye Arslansoy<sup>1</sup> · Lei Sun<sup>3</sup> · Somdutt Mujwar<sup>4</sup>

Received: 7 February 2024 / Revised: 5 June 2024 / Accepted: 18 June 2024 / Published online: 24 June 2024  
© The Author(s), under exclusive licence to Springer Nature Switzerland AG 2024

## Abstract

Human body odor is a result of the bacterial biotransformation of odorless precursor molecules secreted by the underarm sweat glands. In the human axilla, *Staphylococcus hominis* is the predominant bacterial species responsible for the biotransformation process of the odorless precursor molecule into the malodorous 3M3SH by two enzymes, a dipeptidase and a specific C-S lyase. The current solutions for malodor, such as deodorants and antiperspirants are known to block the apocrine glands or disrupt the skin microbiota. Additionally, these chemicals endanger both the environment and human health, and their long-term use can influence the function of sweat glands. Therefore, there is a need for the development of alternative, environmentally friendly, and natural solutions for the prevention of human body malodor. In this study, a library of secondary metabolites from various plants was screened to inhibit the C-S lyase, which metabolizes the odorless precursor sweat molecules, through molecular docking and molecular dynamics (MD) simulation. In silico studies revealed that tannic acid had the strongest affinity towards C-S lyase and was stably maintained in the binding pocket of the enzyme during 100-ns MD simulation. We found in the in vitro biotransformation assays that 1 mM tannic acid not only exhibited a significant reduction in malodor formation but also had quite low growth inhibition in *S. hominis*, indicating the minimum inhibitory effect of tannic acid on the skin microflora. This study paved the way for the development of a promising natural C-S lyase inhibitor to eliminate human body odor and can be used as a natural deodorizing molecule after further in vivo analysis.

**Keywords** *Staphylococcus hominis* · Body malodor · Tannic acid · Molecular docking

## Introduction

Human body odor formation is a combination of odorless precursor secretions from axillary sweat glands and the biotransformation of these precursors into malodorous molecules by a large and mixed population of microorganisms. Once odor precursor molecules are produced and secreted onto the skin surface, the bacterial commensals colonizing the axilla utilize these molecules to produce sulfur-containing compounds (Natsch and Emter 2020). The vast majority of bacterial commensals on the human axilla predominantly consist of gram-positive bacteria, *Staphylococcus*, *Anaerococcus*, *Corynebacterium*, and *Propionibacterium* (Troccaz et al. 2015). It has been discovered that *Staphylococcus* contributes the most to the production of odorous molecules, and of *Staphylococcus* species, *Staphylococcus epidermidis* and *Staphylococcus hominis* are the most abundant species in the axilla microbiota. Particularly, *S. hominis* is the main

---

Ayşe Doga Karipcin, Ayşe Hamide Köse, Ayşe Anaz, and Beyza Nur Demirsoy contributed equally to this work.

✉ Ozkan Fidan  
ozkan.fidan@agu.edu.tr

- <sup>1</sup> Department of Bioengineering, Faculty of Natural and Life Sciences, Abdullah Gül University, 38080 Kayseri, Turkey
- <sup>2</sup> Department of Molecular Biology and Genetic, Faculty of Natural and Life Sciences, Abdullah Gül University, 38080 Kayseri, Turkey
- <sup>3</sup> School of Life Science and Chemical Engineering, Jiangsu Second Normal University, Nanjing 211200, China
- <sup>4</sup> Chitkara College of Pharmacy, Chitkara University, Rajpura, Punjab 140401, India

responsible microorganism for body odor production in humans (Bawdon et al. 2015).

In the human axilla, four major molecular components are identified as the leading cause of body odor. First, the presence of volatile odorous steroid precursors is identified in the male axilla malodor. Second, the contribution of volatile fatty acids (VFAs) to the human axilla sweat odor is the result of the bacterial transformation of precursor molecules by *Corynebacterium* spp (Troccaz et al. 2004). Third, (E)-3-methylhex-2-enoic (3M2H) acid was found to be one of the abundant malodor-causing molecules. Both E- and Z-3M2H are present in the axillary odor secretions, and these constitute greater proportions of the odorous secretions than those of steroids do. It was identified that 3M2H molecules are accompanied by water-soluble proteins during their transportation into the skin (Zeng et al. 1996). Lastly, volatile fatty acids (VFAs) and thioalcohols are the predominant malodor molecules with thioalcohols being the most pungent

molecules (James et al. 2004). For the human body malodor, the main thioalcohol is 3-methyl-3-sulfanylhexan-1-ol (3M3SH). Odor-causing molecule 3M3SH is generated from S-Cys-Gly-3M3SH (S-[1-(2-hydroxyethyl)-1-methylbutyl]-L)cysteinyglycine), a malodor precursor molecule secreted from the human apocrine glands (Fig. 1).

It was recently discovered that the biotransformation of the secreted malodor precursors to thioalcohol is catalyzed by the activity of a dipeptidase and a specific C-S lyase (Rudden et al. 2020). In the process of 3M3SH biotransformation, S-Cys-Gly-3M3SH molecule is first transported into the *S. hominis* by a proton-coupled peptide transporter, a member of the proton-coupled oligopeptide transporter (POT) family named PepTSh. Due to the specific binding pocket of the transporter, it can easily recognize thioalcohol groups (Minhas et al. 2018). Following the uptake into the bacteria, the S-Cys-Gly-3M3SH molecule is first exposed to the  $\beta$ -elimination process to remove the glycine by a

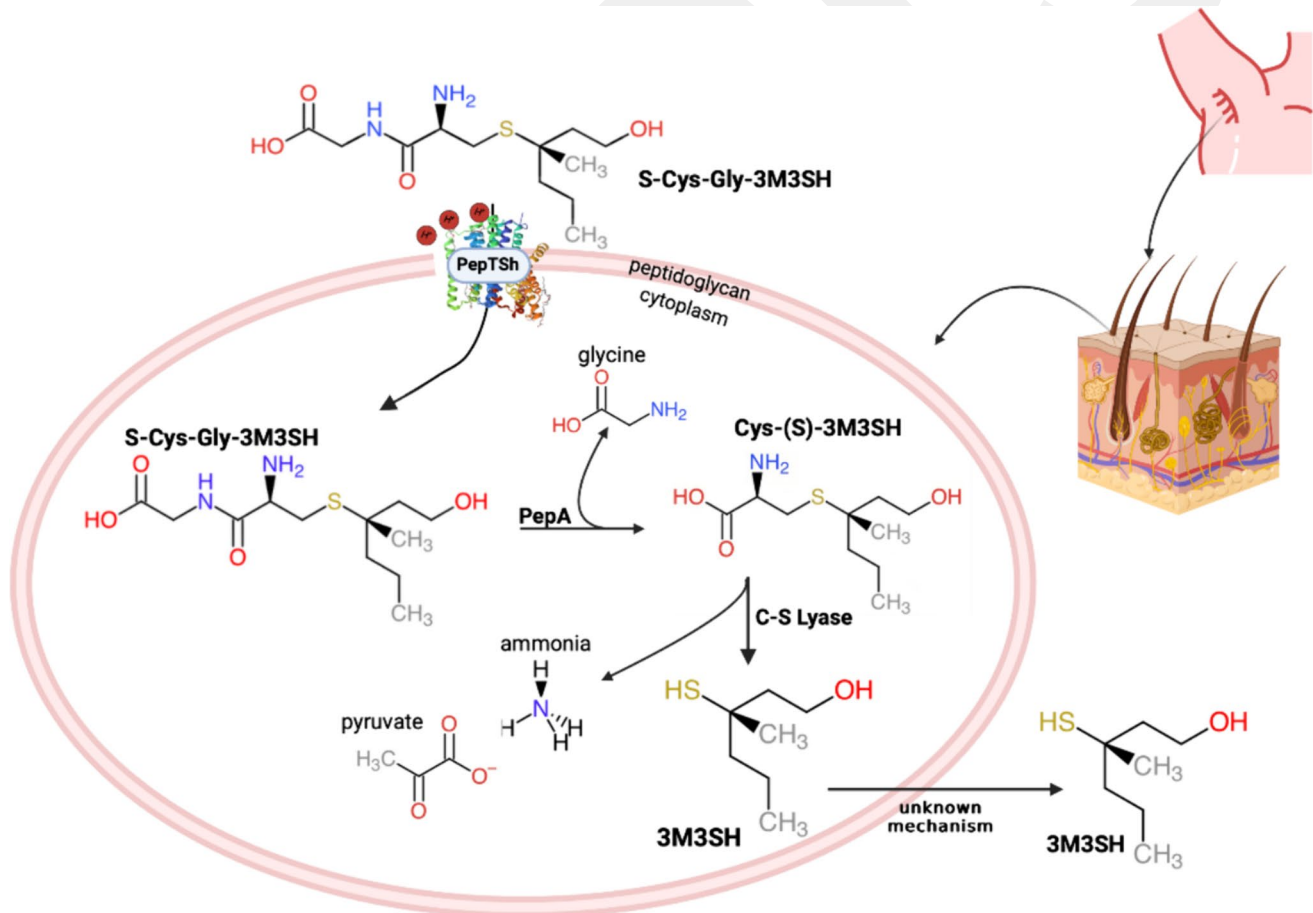


**Fig. 1** Malodorous thioalcohol production process in *S. hominis*. The secreted precursor, S-Cys-Gly-3M3SH, is first transported into the cytoplasm of *S. hominis* via the PepTSh transporter which is facilitated by a proton co-transportation. Then, the  $\beta$ -elimination reaction, in which the terminal glycine of Cys-Gly-3M3SH is cleaved by a

dipeptidase, PepA, takes place to produce Cys-3M3SH. Subsequently, cysteine residue is cleaved by a specific C-S lyase, ShPatB, generating the odorous free-thioalcohol (3M3SH) along with liberated ammonia and pyruvate. The free thioalcohols are released outside the cell by an unknown mechanism

dipeptidase, PepA, which is commonly found in all staphylococcal subspecies. Moreover, the cleavage of the precursors by the lyase is a unique step in body malodor production. It was identified as an uncommon C-S lyase, named ShPatB, for the cleavage of Cys-3M3SH. Due to the hydrophobic pocket of ShPatB, the enzyme can recognize Cys-3M3SH with higher affinity (Rudden et al. 2020). As the cysteine residue of the precursor is cleaved by the ShPatB in the cytoplasm of *S. hominis*, the malodorous molecule 3M3SH is produced. It is, then, secreted into the skin by an unknown mechanism (Fig. 1) (Minhas et al. 2018).

To suppress the pungent sweat odor, several cosmetic products such as deodorants and antiperspirants are often preferred. However, such cosmetic products mask the undesired malodor by either blocking the apocrine glands or disrupting the microbiota. Conventional deodorants and antiperspirants are widely used but come with a set of challenges that have driven the demand for alternative solutions. These challenges include their limited effectiveness over time, reliance on potentially harmful chemical ingredients, inadequate performance for individuals with specific needs such as hyperhidrosis, and their negative impact on the environment (Teerasumran et al. 2023). Furthermore, they contain various chemicals that endanger both the environment and human health. Of these chemicals, triclosan has a detrimental effect on aquatic microorganisms and bioaccumulation in food (Oliveira et al. 2021). In addition, because of the inhibition of apocrine ducts to secrete odorless precursors, the application of such products for a long period of time can have an effect on the function of sweat glands and even may lead to loss of function (Benohanian 2001). With an increase in estrogen alpha-receptor due to long-term aluminum exposure from these products, a greater likelihood of cancer was reported (Gorgogietas et al. 2018). Consequently, there is a growing interest in novel approaches to address body odor, and one promising avenue is targeting C-S lyase enzymes within the skin's microbiome. This innovative approach seeks to mitigate body odor by modulating the breakdown of sulfur-containing compounds found in sweat, addressing the issue at its source. Moreover, focusing on C-S lyase aligns with the broader societal shift towards sustainable and personalized solutions, potentially reducing the environmental footprint associated with conventional deodorants while providing more effective and tailored alternatives for individuals.

For centuries, people have been traditionally using various types of natural substances such as lemon, green tea, and coconut oil in order to address this issue. In the recent times, extensive efforts have been devoted towards the exploration of herbal medicine as alternative medicine therapy and because of their widespread utilization, medicinal plants are considered to be most valuable assets of the ecosystem to develop newer therapeutics for patient healthcare system

since the dawn of time, and because of their basic therapeutic curative role, they continue to play an essential role in modern times. The rise in the recognition of medicinal plants as a source of therapeutics and other products is largely due to their efficacy, and as a cost-effective alternative to high-priced synthetic drugs (Watal et al. 2014; Behl et al. 2021). Thus, in this study, we generated and screened 168 plant-based secondary metabolites from the traditional natural solutions against the active site of the ShPatB using *in silico* techniques involving molecular docking and molecular dynamics (MD) simulation. *In silico* results revealed that three molecules (tannic acid, gossypetin, and nimbadiol) had the strongest binding affinities to the target enzyme. Particularly, the stable binding ability of tannic acid to ShPathB was also confirmed in the MD simulation. Additionally, the tannic acid was tested *in vitro*, in which a structural analog of Cys-3M3SH, namely L-felinine which is putative pheromone precursor of cat urine (Miyazaki et al. 2006) and displays very similar enzymatic activity (Rudden et al. 2020), was used as a non-odorous precursor molecule. The *in vitro* biotransformation assay results indicated that tannic acid at certain concentrations led to the significant inhibition of malodor formation with minimum antimicrobial activity against *S. hominis*, suggesting that this natural product is a promising candidate for preventing the sweat malodor with a C-S lyase inhibitory activity.

## Materials and methods

### Molecular docking

The crystal structure of C-S lyase (6QP1) was retrieved from the Protein Data Bank (PDB). Only the A chain (chain A) of C-S lyase, which has a homodimeric structure, was used for molecular docking by removing the other chain from the macromolecular structure. Prior to docking, defining active binding sites, exclusion of water molecules, the addition of polar hydrogens, and arrangement of Kollman charges (Owen et al. 2023) were performed by using the “MGL tool” program version 1.5.6. (Goddard et al. 2018). The sphere that covered the binding site was maintained at fixed coordinates by covering the extended conformations of the reference ligand, and polar hydrogens were added to the structure and saved in \*.pdbqt format by using AutoDock 4.2 tool (Morris et al. 2009). Then, a natural product-based ligand library was created by downloading their three-dimensional chemical structures of the molecules from the “PubChem” database in sdf format (Table S1). The energy minimization of the files downloaded ligands was performed by using the Rdkit program. Selected ligands were converted from sdf format to pdbqt format using the Open Babel program for

the execution of docking analysis (García-Ortegón et al. 2022). Molecular docking was executed by using “Autodock Smina,” an enhanced version of the “Autodock Vina” program. Docking protocol was validated by redocking the co-crystallized reference ligand within the macromolecular cavity and superimposing the docked conformation with its bioactive crystallized conformation. For the concerned macromolecular target, the ligand with the best docking result was shortlisted (Masters et al. 2020). Autodock software uses Lamarckian genetic algorithm (LGA) as a primary conformational search for molecular docking simulation. A large number of possible conformations were generated for selecting individuals with lowest binding energy. The individual conformational search for its local conformational space, discovering local minima and then proceed this information to later generations is performed by “Lamarckian” aspect, which is its additional feature. The binding energy of the small molecules with macromolecular targets is predicted by using the semi-empirical force field (Agrawal et al. 2021; Kciuk et al. 2022; Fidan and Mujwar 2024). AutoDock 4.2 tool was also used for the calculation of inhibition constants ( $K_i$ ) for hit molecules (Khan et al. 2019). The interactions of enzymes and ligands were visualized by using “PyMOL2” and “Discovery Studio” softwares.

### Molecular dynamics simulation

Molecular dynamics (MD) simulation of the C-S lyase of *S. hominis* complexed with tannic acid was performed for 100 ns with the Desmond module of the Schrödinger program version 2021-4 to assess the binding stability and patterns of the tannic acid within the macromolecular target site by using OPLS3e force field (Shah et al. 2020; Mujwar 2021; Fidan et al. 2023). The single point charge (SPC) model was used to infer the water molecules with an orthorhombic-shaped simulation box, a 10 Å gap was left between the wall and the tannic acid-protein complex, and counter ions were injected using 0.15 M NaCl to neutralize the existing charge. The long-range electrostatic connections between the macromolecule and the complexed ligand were computed by applying the particle-mesh Ewald (PME) method with 0.8 grid spacing and a cutoff radius of 9.0 for Coulomb interactions after the NPT ensemble MD simulation was run for 100 ns. Following that, 2000 iterations were performed using a merging threshold of 1 kcal/mol to decrease the system’s energy. Then, over the next 100 ns, a constant temperature of 300 K and pressure of 1.013 bar were maintained. To create simulation interaction graphs, the trajectory route was set to 9.6 with an energy interval of 1.2 ps after the simulation process was completed (Mujwar et al. 2021, 2022; Fidan 2022; Shinu et al. 2022).

### Bacterial strains and chemicals

*S. hominis* B10 strain was kindly provided by a researcher Matthew Rose at University of York. 5,5-dithio-bis-(2-nitrobenzoic acid) (DTNB, Ellman’s Reagent) was kindly provided by a researcher at Harran University. Tannic acid and L-felinine were purchased from Shanghai Aladdin Bio-chem Technology Co. Ltd. The stock solution of L-felinine was prepared at 80 mM concentration in DMSO and stored in 4 °C until used. The stock solution of tannic acid was prepared at 40 mM concentration in DMSO and stored at 4 °C until used. The stock solutions of 2 mM DTNB with 50 mM sodium acetate and Tris-HCl were prepared in sterile dH<sub>2</sub>O. The solution pH was set to 8. LB medium was utilized for the growth of *S. hominis*, while M9 minimal medium was used for the in vitro biotransformation assays.

### In vitro biotransformation assay

*S. hominis* B10 strain was inoculated from a pure colony and grown overnight in LB. Optical density measurements at 600 nm were performed in the spectrophotometer (Genesys 10s UV-Vis Thermo Scientific) to measure the cell density. Afterward, bacterial cells were harvested and subsequently suspended in the appropriate volume of M9 medium to reach a final OD<sub>600nm</sub> of 10. Variable concentrations of tannic acid (0.5 mM, 1 mM, 2 mM, 4 mM) from a 40 mM tannic acid stock solution were used in biotransformation reactions, and the bacterial cells in M9 medium, tannic acid, and L-felinine with their corresponding amounts were added to sterile microcentrifuge tubes (Table S2). Cells and tannic acid-only (no added substrate) reactions were also performed as positive controls. All reactions were triplicated and incubated at 37 °C for 5 h.

To measure the released thioalcohol yield quantitatively, the samples were centrifuged at 13,000 rpm for 2 min. One hundred microliters of supernatant from each reaction, 100 µl DTNB, and 100 µl Tris-HCl (pH 8.0) were added into sterile microcentrifuge tubes by completing the total volume to 1000 µl with sterile distilled water. The reactions were incubated at room temperature for 5 min. Then, the OD<sub>412nm</sub> for each reaction was measured (Bawdon et al. 2015).

### Antimicrobial susceptibility assay

Tannic acid solutions were prepared from the 40 mM stock solution as followed: 0.5 mM tannic acid, 1 mM tannic acid, and 2 mM tannic acid were diluted with ethanol to a total final volume of 20 µl. Four millimolar tannic acid was prepared with ethanol to a total final volume of 50 µl. Ten microliters of diluted tannic acid solutions in ethanol was added to sterile paper discs and dried. This step was repeated until all the solutions were absorbed by the discs.

One hundred microliters of ethanol as a negative control and 10  $\mu$ l of 100-mg/mL ampicillin as a positive control were added to the paper discs as described above. *S. hominis* was spread on an LB agar plate, and after the paper discs completely dried, they were placed on the plate. Following the overnight incubation at 37 °C, the diameter of the zone of inhibitions for each disc was measured. All the procedures for disc diffusion assay were performed in triplicate.

### Statistical analysis

All measurements were performed in triplicates, and data is analyzed statistically by one-way paired *t* test using GraphPad Prism (version 8.0.2).

## Results

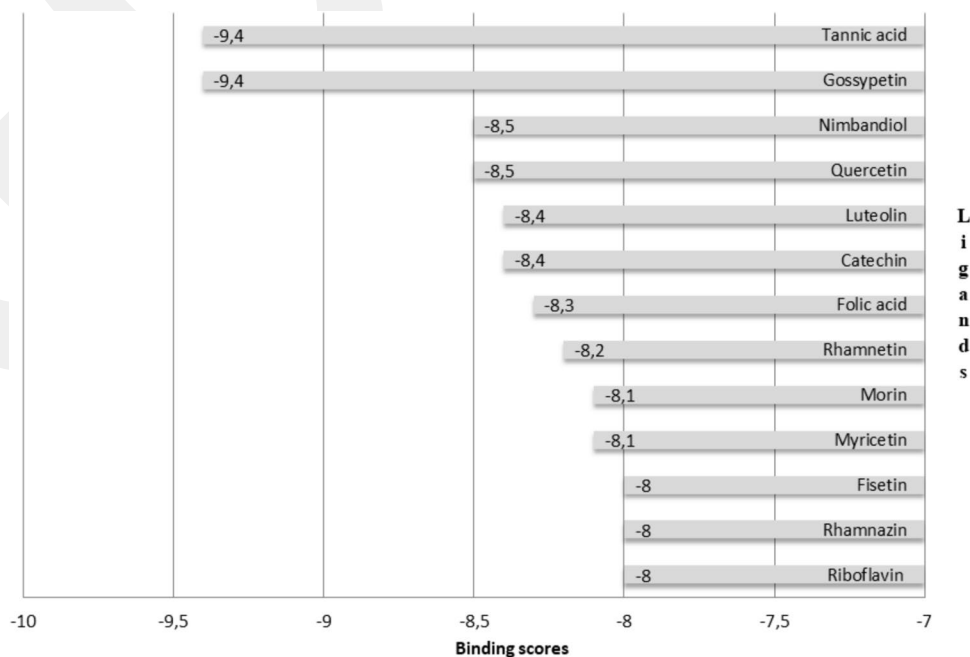
### Molecular docking

Molecular docking-based screening of plant-based ligand library from traditional natural products was performed against bacterial C-S lyase to determine the most effective natural inhibitor to prevent body malodor formation. In addition to traditionally used molecules, a detailed literature review was conducted to propose a natural molecule that would inhibit C-S lyase. Chamomile is one of the plants frequently used for natural treatment. It is used for skin conditions such as eczema, it also has anti-inflammatory characteristics and deodorizing effects (Gardiner 1999). Similarly, due to its anti-fungal and anti-inflammatory effect,

tea tree oil is used for deodorizing effects in antiperspirants and deodorants with low concentrations (Priest 1999). The most common plant that is used to suppress the smell is lemon. The acidic properties of fruit lemon have anti-inflammatory effect (El-Desoukey et al. 2021). It stops odor by killing the bacterial population. Furthermore, coconut oil is used as an ingredient in natural deodorants because of its antibacterial characteristics (Ng et al. 2021). The secondary metabolites from the traditional natural substance were extracted from the literature, led to the creation of the ligand library with 168 molecules. ChemDraw15 was used to draw all 2-D chemical structures (ChembridgeSoft Corporation, MA, USA). Marvin Sketch 5.3.7, Chem Axon, was used to convert these 2D structures into stabilized 3D conformation followed by the energy minimization process. MGLTools 1.5.6.rc1 was used to parametrize all structures (ligands) (Mujwar and Tripathi 2022; Shinu et al. 2022). Docking protocol was successfully validated as the docked conformation of the co-crystallized reference ligand was perfectly superimposed over its bioactive crystallized conformation. The perfectly overlaid conformation of the docked conformation of the co-crystallized reference ligand over its bioactive conformation is shown in Fig. S1.

The molecular docking of 168 ligands was performed against C-S lyase, and the binding energy scores for all ligands were listed in Table S1. The ligands with the lowest binding energy scores were shortlisted in Fig. 2 using  $-8$  kcal/mol as the threshold. Particularly, tannic acid and gossypetin had the lowest binding energy of  $-9.4$  kcal/mol, and its dissociation/inhibition constant ( $K_i$ ) value was found to be 126.41 nM. They were followed by nimbandiol and

**Fig. 2** The binding scores of the ligands docked against C-S lyase. The threshold was set to  $-8$  kcal/mol



quercetin with binding energy scores of  $-8.5$  kcal/mol with  $K_i$  value of 578.42 nM. In this study, tannic acid was further shortlisted to confirm the stability of the ligand in the binding pocket of the target protein through MD simulation since the cost and the accessibility of the gossypetin are very high and relatively difficult. Moreover, considering the economic contributions of the inexpensive natural product in potential cosmetic product formulations to be made in the future, MD simulations and experimental procedures with tannic acid were chosen for further in silico and in vitro analysis.

### Molecular dynamics simulation

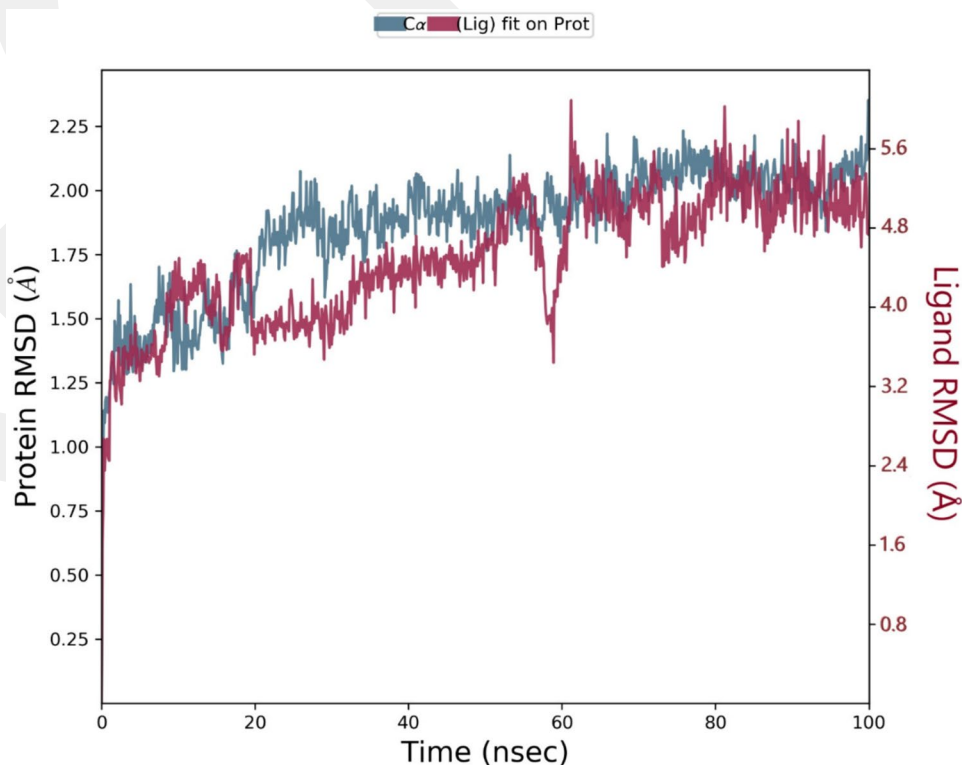
The C-S lyase of *S. hominis* complexed with the ligand was found to be highly stable throughout the simulation process. The C-S lyase of *S. hominis* was made up of 386 amino acids, while the complexed ligand is having 11 rotatable bonds and 122 heavy atoms out of a total of 170 atoms. The RMSD was used to calculate the stability and structural changes of the protein backbone. During the simulations, the complex was shown to be stable with an average RMSD for the macromolecular backbone ranging from 1.25 to 2.0 Å, while tannic acid remained stable throughout with very little fluctuation inside the receptor's cavity with the RMSD ranging from 4.0 to 5.6 Å throughout the simulation process (Fig. 3).

The RMSF of the target receptor was also calculated by measuring the change of C $\alpha$  atoms within the peptide chain

to quantify the vibrations of the amino acids relative to their original conformations. The RMSF value of the macromolecular backbone of C-S lyase of *S. hominis* was discovered to be between 0.5 and 1.5 Å. Following the investigation, it was discovered that the RMSF for the active amino acids was lower for the complex system and that the complexed ligand mean alteration was in the range of 1.0–6.0 Å, suggesting that the ligand took a couple of moves within the macromolecular cavity to achieve its most stabilized conformation. Fig. 4 depicts the RMSF of the C-S lyase C $\alpha$  backbone as well as complex ligands detected over the 100-ns period of MD simulation.

The SSE analysis revealed that the macromolecular structure of C-S lyase of *S. hominis* included 47.56% SSE, with 33.84% alpha-helices and 13.72% beta-sheets remaining constant during the MD simulation. The stability of tannic acid in the target macromolecule was determined by measuring the strength of hydrogen bonds, hydrophobic contacts, and ionic interactions created throughout the simulation procedure. Furthermore, 2D and 3D interactions of tannic acid with C-S lyase were investigated during the simulation and demonstrated in Fig. 5. The results showed that the tannic acid was hydrophobically attached to the amino acids Tyr25, Tyr132, Lys246, and Ala251; whereas Asp15, Met17, Glu20, Asp140, Met254, and Glu362 via forming hydrogen bonds, and residues Ala47, Asp48, Asn249, Ile250, Gly252, Phe255, Thr276, Asn278 were engaging with complexed ligand through forming a water bridge (Fig. 6).

**Fig. 3** RMSD of the ligand, as well as C $\alpha$ -backbone of C-S lyase of *S. hominis*, complexed with tannic acid measured over 100 ns of MD simulations



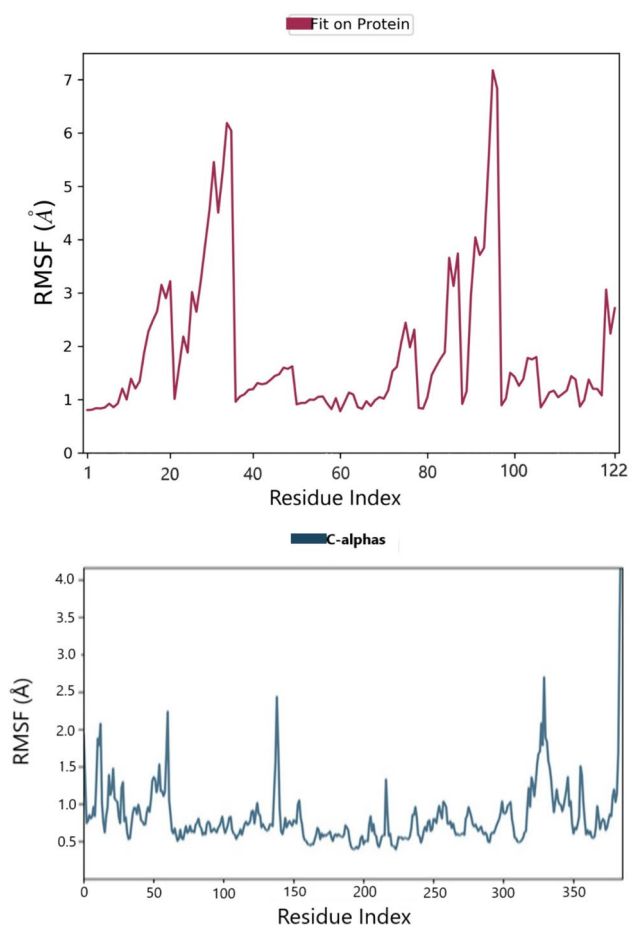


**Fig. 4** RMSF of the C-S lyase of *S. hominis* and its complex with tannic acid was assessed after conducting an MD simulation for 100 ns

### Effects of tannic acid at various concentrations on the inhibition of C-S lyase

In order to quantify the extent to which different concentrations of tannic acid interfere with the C-S lyase of *S. hominis*, we spectrophotometrically measured the DTNB-labeled thioalcohol production at 412 nm. Based on the average absorbance values, when the biotransformation reactions were treated with 1 mM tannic acid, the production of thioalcohol was dropped by 94%, indicating the highest efficacy in the inhibition of C-S lyase. The concentrations of tannic acid at 0.5 mM, 2 mM, and 4 mM generated 33%, 84%, and 88% reduction in thioalcohol yield, respectively (Fig. 7A). These results are in line with the statistical analyses. The data was subject to a one-way paired *t* test, and the significance threshold was set at 0.05. Tannic acid concentrations at 1 and 2 mM exhibited greater significance when compared to the control group. At this juncture, it is vital to assess the effect of different concentrations of tannic acid on bacterial viability. Therefore, an antimicrobial susceptibility assay was performed in order to determine the concentration

at which tannic acid is most efficient in the inhibition of C-S lyase of *S. hominis*, but has the minimum effect on the growth of *S. hominis*.

### Antimicrobial susceptibility assay

The impact of tannic acid on the survival of bacterial cells was evaluated by measuring the zone of inhibition observed around the discs which were impregnated with different concentrations of tannic acid (0.5 mM, 1 mM, 2 mM, 4 mM) and placed on *S. hominis* spread LB Agar plate. It has been shown that at various concentrations, tannic acid influenced cell viability. As seen in Fig. 7B and Fig. S2, a higher concentration of tannic acid resulted in a larger diameter of the zone of inhibition, which is proportional to the antimicrobial activity of the compound.

Based on the *in vitro* biotransformation assay, 1 mM tannic acid was determined as the most efficient concentration to inhibit C-S lyase (*p* value 0.001). Since the higher concentrations have significant antimicrobial effect on cells and suggesting that it may damage microflora when used as a deodorizing compound, use of lower concentrations of tannic acid is necessary to protect microflora. Therefore, 1 mM tannic acid was determined as the most optimum concentration by considering both the inhibitory effect of tannic acid on the target enzyme and its antimicrobial activity on cells to prevent biotransformation of S-Cys-Gly-3M3SH to malodorous thioalcohol by C-S lyase while preserving the microflora.

### Discussion

The presence of body odor is a result of the enzymatic reactions in bacteria found in the axillary microbiota. C-S lyase converts the precursor Cys-Gly-3M3SH thioalcohol into 3M3SH, which is the predominant volatile molecule leading to body odor in humans. Although there are different species responsible for this biotransformation, the main contributor is *S. hominis* (Rudden et al. 2020). In this study, our focus was to target C-S lyase in *S. hominis* as a way to reduce body malodor formation because, to our knowledge, natural products have not been tested against C-S lyase. The cosmetic industry is largely shifting from chemical additives to enzyme-based solutions due to potential adverse effects of these ingredients on the skin and health conditions. Therefore, need for safer and more effective skin products in cosmetic industry has accelerated the research to reveal enzyme-based alternatives for replacing active chemicals in cosmetic formulations (Sung et al. 2019). The present study addresses this current problem in the context of safer and more effective anti-odor products from natural sources. For this purpose, the natural product library was formed

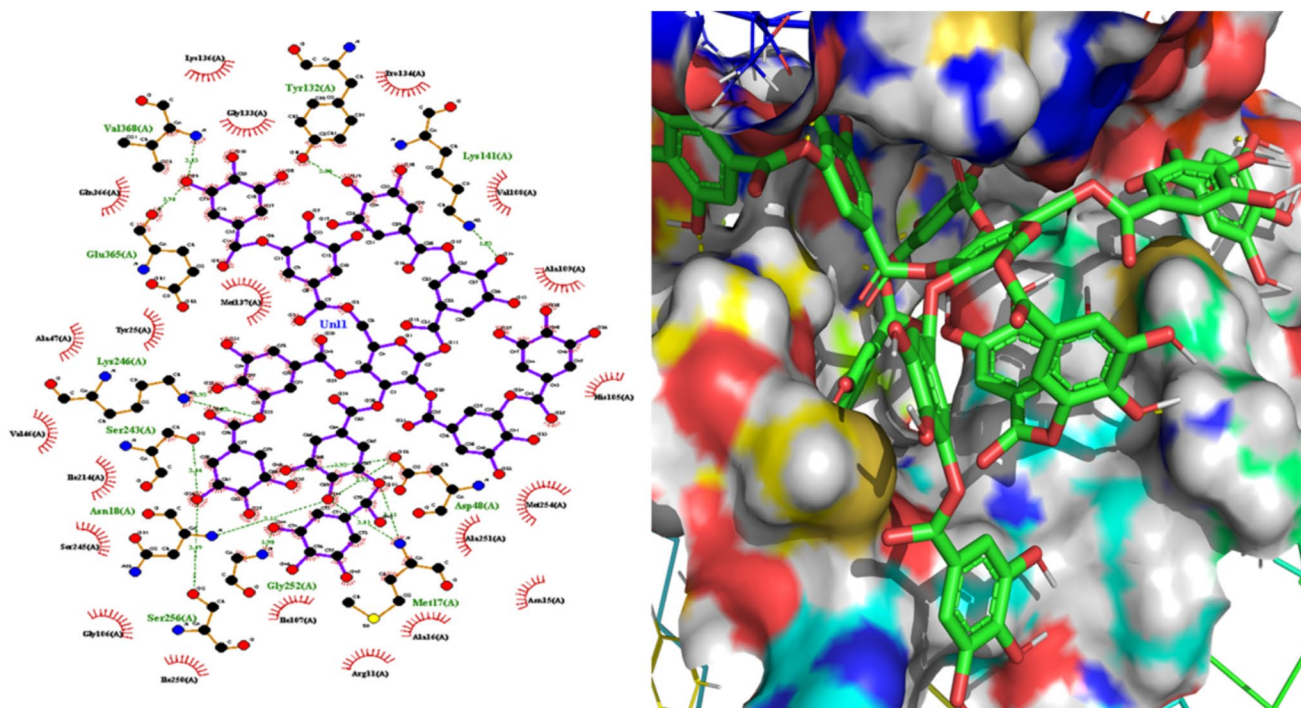
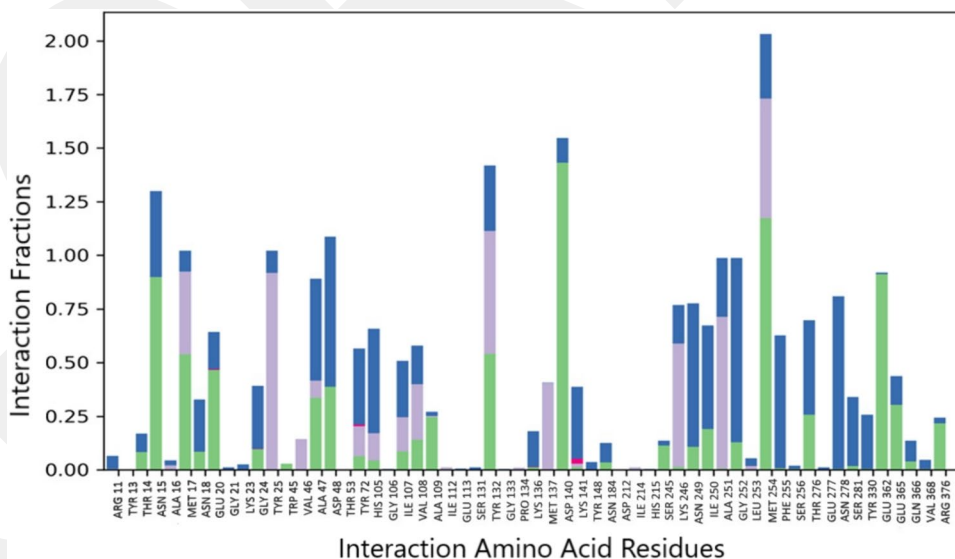


**Fig. 5** **A** Two-dimensional interactions of tannic acid against C-S lyase of *S. hominis* observed during a 100-ns MD simulation. **B** 3D visualization of C-S lyase-tannic acid complex

**Fig. 6** Protein-ligand contacts observed between the C-S lyase of *S. hominis* and complexed ligand during a 100-ns MD simulation. Hydrogen bonds are shown as green bars, water bridges as blue bars, and hydrophobic interactions as purple bars



from the natural substances traditionally used to prevent body malodor. The virtual screening of the ligand library against C-S lyase led to the discovery of potential inhibitor molecules with strong binding affinities. The majority of the hit molecules are polyphenolic compounds, dominantly flavonoids. Among them, tannic acid and gossypetin had the lowest binding energy scores. Tannic acid and flavonoids, specifically quercetin, showed similar biological activities

such as anti-biofilm and anti-inflammatory effects. They both also displayed a therapeutic effect in atopic dermatitis (Park et al. 2006; Rogerio et al. 2007; Jung et al. 2010; Lee et al. 2013). Thus, it is expected to have similar binding scores of flavonoids and tannic acid. In addition, following in silico studies, we have decided to exclude gossypetin from in vitro tests due to its high cost. On the other hand, tannic acid with versatile bioactivities is easily available and cheap

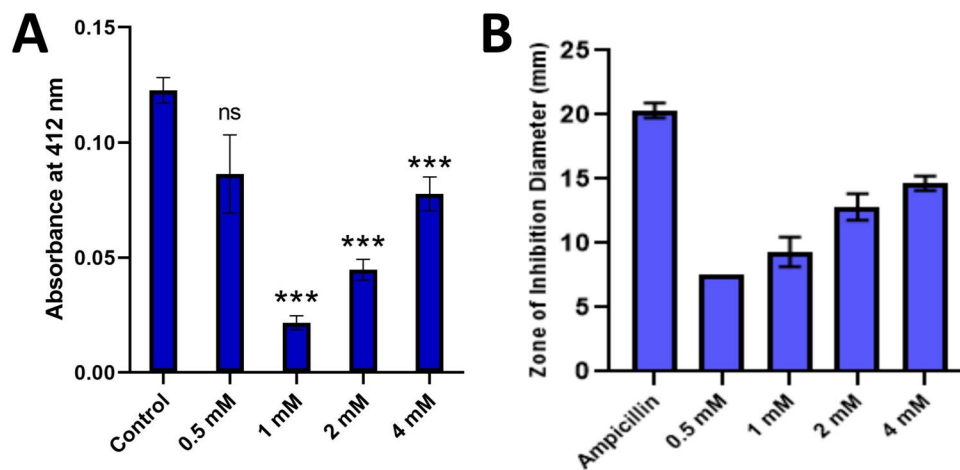


**Fig. 7** **A** The comparison of absorbance values of DTNB-labeled thioalcohol yield between the control group and the four concentrations of tannic acid (TA) measured by the spectrophotometer at 412 nm. One-way paired *t* test performed; ns, *p* value  $> 0.05$ ; \*\*\**p* value  $< 0.0005$ . Threshold set as *p* value  $< 0.05$ , and the most efficient con-

centration determined as 1 mM with *p* value 0.0001 while 2 mM and 4 mM have *p* value 0.0003. **B** The zone of inhibition diameter (mm) of tannic acid concentrations (0.5 mM, 1 mM, 2 mM, 4 mM) and ampicillin as the control group

natural product for the development of affordable natural cosmetic product. Therefore, the MD simulations for tannic acid complexed with C-S lyase was performed for 100 ns. Tannic acid structure has a central glucose molecule attached to ten gallic acid molecules. The reason why tannic acid showed the highest affinity is that higher enzyme suppression occurs in the presence of aryl residue linked to two vicinal hydroxyl groups which found in the tannic acid structure (Egert et al. 2013). This correlation has been demonstrated through the application of the molecular dynamics method, which confirmed the stability of tannic acid in the binding pocket of C-S lyase during 100-ns simulation. The docking-based screening revealed that the tannic acid showed best binding energy of  $-9.4$  kcal/mol for the bacterial C-S lyase enzyme, and thus the macromolecular complex of tannic acid within the active site of the concerned target was shortlisted to execute MD simulation for 100 ns to reveal their thermodynamic stability with time. The MD analysis have revealed that the tannic acid remains highly stabilized within the macromolecular cavity throughout the simulation with the RMSD value in the range of 4.0–5.5 Å, while the RMSF value was also observed within the range of 0.5–2.0 Å indicating very low fluctuation with high degree of thermodynamic stability. Also, the tannic acid was found to be interacting with good number of key macromolecular residues throughout the simulation via hydrogen bonding, van der Waal's forces, and alkyl interactions contributing to their stabilized binding. While in the other hand, the macromolecular backbone remained stabilized without any fluctuation or conformational change required to initiate their bioactivity. Therefore, by analyzing the observed docking and MD simulation results, it was concluded that the tannic

acid is a competitive inhibitor of the bacterial C-S lyase enzyme, and the same has been validated by performing in vitro assay.

The inhibition characteristics of the tannic acid were tested by in vitro biotransformation assay, and the statistical analyses revealed that both 1 mM, 2 mM, and 4 mM tannic acid show significant inhibition of the odor-causing molecule. Since the human axilla consists of various species, it is required to further investigate the effect of tannic acid on axillary microbiota. For this reason, antimicrobial susceptibility assay was performed to establish a potential risk for disrupting the bacterial populations. Previous studies revealed that a concentration of 20 μM tannic acid does not exhibit inhibitory effects on the growth of *S. aureus*, one of the bacterial species found in axillary microbiota. While tannic acid demonstrated its antibacterial characteristics against both Gram-positive and Gram-negative bacteria, there is a scarcity of preclinical and clinical studies addressing the efficacy of tannic acid against bacterial infections (Payne et al. 2013). The results of the antimicrobial susceptibility assay indicated that lower concentrations of tannic acid have shown less bacterial disruption. Therefore, 1 mM tannic acid has been chosen as the best candidate for enzymatic inhibition in *S. hominis* with the most significant *p* value (0.0001) and less antimicrobial activity.

This study establishes the potential of tannic acid, a natural phenolic compound found in herbaceous and woody plants such as nutgalls, as an anti-odor agent against sweat glands. Tannic acid has various biological activities such as antimicrobial, antiviral, anti-cancer, and antioxidant (Kaczmarek 2020). For instance, it exhibited a great potential as chemotherapeutic agent by blocking cancer-feeding

pathways while promoting the activity of tumor-suppressive elements (Youness et al. 2021). Another beneficial effect of tannic acid is its antioxidant activity. It is established that tannic acid has a protective influence on cells against oxidative lesions (Perumal et al. 2019). Additionally, tannic acids show restorative impacts against neurological and cardiovascular damage (Jing et al. 2022). However, the applications of tannic acid are not yet fully developed due to low lipid solubility and its limited bioavailability (Youness et al. 2021). The deodorizing effect of chestnut inner shell extracts (CISE) containing tannins and flavonoids was tested against trans-2-nonenal and methyl mercaptan which are odorous compounds. It was found that inhibition of the odor is positively correlated with the concentration of CISE (Ham et al. 2015). In this study, an extract was used, yet tannic acid was not directly tested for its potential deodorizing activity. Furthermore, tannic acid was also reported to significantly prevent the production of fishy smell-related volatile components such as heptanal and (E, E)-3, 5-octadiene-2-one (Wang et al. 2023). This recent study clearly indicated the potential of tannic acid in blocking the odor due to a variety of molecules. In our study, we not only extended the odor blocking spectrum of tannic acids to thioalcohols, but also revealed its inhibitory role in the odor formation process of *S. hominis* by blocking C-S lyase.

## Conclusion

This article investigated a natural-based solution to inhibit odor-causing enzyme from *S. hominis* due to concerns about the environmental and health impacts of commonly used cosmetic products like deodorants and antiperspirants. Molecular docking analysis identified tannic acid as a potent inhibitor, confirmed by biotransformation assays. Tannic acid at 1 mM concentration yields the maximum inhibitory effect on the C-S lyase of *S. hominis* with less intervention on bacterial viability. Therefore, this study proposes tannic acid as a promising candidate in the field of natural-based cosmetics, offering both deodorant efficacy and microbiota-friendly properties, along with economic benefits. Furthermore, this study paves the way for the development of a promising natural C-S lyase inhibitor, tannic acid, for the elimination of human body odor and can be used as a natural deodorizing molecule. Future investigations, including in vivo and clinical studies, are crucial to comprehensively assess tannic acid's impact on the microbiota.

**Supplementary Information** The online version contains supplementary material available at <https://doi.org/10.1007/s10123-024-00551-5>.

**Acknowledgements** The authors would like to thank Matthew Rose (University of York, UK) for providing *S. hominis* B10. The authors

also thank Huseyin Guner (Abdullah Gul University) for performing molecular docking.

**Author contribution** Ayse Doga Karipcin, Ayse Hamide Kose, Ayse Anaz, Beyza Nur Demirsoy, Nuriye Arslansoy, and Somdutt Mujwar conducted the experiments. Ozkan Fidan designed the research study. Somdutt Mujwar and Lei Sun contributed essential reagents and tools. Somdutt Mujwar and Nuriye Arslansoy analyzed the data. Ayse Doga Karipcin, Ayse Hamide Kose, Ayse Anaz, Beyza Nur Demirsoy, Nuriye Arslansoy, Somdutt Mujwar, and Ozkan Fidan wrote and revised the manuscripts.

**Funding** This study was funded by the TUBITAK under 2209-A University Students Research Projects Support Program 2022/1 (Project N: 1919B012206639).

**Data availability** All data generated in this study are contained in the manuscript and in the supplementary file.

## Declarations

**Conflict of interest** The authors declare no competing interests.

## References

- Agrawal N, Mujwar S, Goyal A, Gupta JK (2021) Phytoestrogens as potential antiandrogenic agents against prostate cancer: an in silico analysis. *Lett Drug Des Discov* 19:69–78. <https://doi.org/10.2174/1570180818666210813121431>
- Bawdon D, Cox DS, Ashford D et al (2015) Identification of axillary *Staphylococcus* sp. involved in the production of the malodorous thioalcohol 3-methyl-3-sufanylhexan-1-ol. *FEMS Microbiol Lett* 362:111. <https://doi.org/10.1093/FEMSLE/FNV111>
- Behl T, Kumar K, Brisc C et al (2021) Exploring the multifocal role of phytochemicals as immunomodulators. *Biomed Pharmacother* 133:110959. <https://doi.org/10.1016/J.BIOPHA.2020.110959>
- Benohanian A (2001) Antiperspirants and deodorants. *Clin Dermatol* 19:398–405. [https://doi.org/10.1016/S0738-081X\(01\)00192-4](https://doi.org/10.1016/S0738-081X(01)00192-4)
- Egert M, Höhne HM, Weber T et al (2013) Identification of compounds inhibiting the C-S lyase activity of a cell extract from a *Staphylococcus* sp. isolated from human skin. *Lett Appl Microbiol* 57:534–539. <https://doi.org/10.1111/LAM.12146>
- El-Desoukey RMA, Al-Qahtani AM, Alqhtani MA et al (2021) Comparative antimicrobial studies between commercial deodorants, alum, sodium bicarbonate and lemon against sweat odor bacteria. *Cohesive J Microbiol Infect Dis* 4:1–5. <https://doi.org/10.31031/CJMI.2021.04.000597>
- Fidan Ö (2022) Investigation of antiviral potential of food carotenoids and apocarotenoids against RNA-dependent RNA polymerase of hepatitis C virus. *Bitlis Eren Üniversitesi Fen Bilim Derg* 11:931–942. <https://doi.org/10.17798/BITLISFEN.1161170>
- Fidan Ö, Mujwar S (2024) In silico evaluation of the potential of natural products from chili pepper as antiviral agents against Dna-directed Rna polymerase of the Monkeypox virus. *Bitlis Eren Üniversitesi Fen Bilim Derg* 13:277–291. <https://doi.org/10.17798/BITLISFEN.1388403>
- Fidan O, Mujwar S, Kciuk M (2023) Discovery of adapalene and dihydrotachysterol as antiviral agents for the Omicron variant of SARS-CoV-2 through computational drug repurposing. *Mol Divers* 27:463–475. <https://doi.org/10.1007/S11030-022-10440-6/FIGURES/5>
- García-Ortegón M, Simm GNC, Tripp AJ et al (2022) DOCK-STRING: easy molecular docking yields better benchmarks for

- ligand design. *J Chem Inf Model* 62:3486–3502. [https://doi.org/10.1021/ACS.JCIM.1C01334/ASSET/IMAGES/LARGE/CI1C01334\\_0013.JPEG](https://doi.org/10.1021/ACS.JCIM.1C01334/ASSET/IMAGES/LARGE/CI1C01334_0013.JPEG)
- Gardiner P (1999) Chamomile (*Matricaria recutita*, *Anthemis nobilis*). Longwood Herb task force:1–21
- Goddard TD, Huang CC, Meng EC et al (2018) UCSF ChimeraX: meeting modern challenges in visualization and analysis. *Protein Sci* 27:14–25. <https://doi.org/10.1002/PRO.3235>
- Gorgogietas VA, Tsialtas I, Sotiriou N et al (2018) Potential interference of aluminum chlorohydrate with estrogen receptor signaling in breast cancer cells. *J Mol Biochem* 7:1
- Ham JS, Kim HY, Lim ST (2015) Antioxidant and deodorizing activities of phenolic components in chestnut inner shell extracts. *Ind Crops Prod* 73:99–105. <https://doi.org/10.1016/J.INDCR.OP.2015.04.017>
- James AG, Hyliands D, Johnston H (2004) Generation of volatile fatty acids by axillary bacterial. *Int J Cosmet Sci* 26:149–156. <https://doi.org/10.1111/J.1467-2494.2004.00214.X>
- Jing W, Xiaolan C, Yu C et al (2022) Pharmacological effects and mechanisms of tannic acid. *Biomed Pharmacother* 154:113561. <https://doi.org/10.1016/J.BIOPHA.2022.113561>
- Jung MK, Hur DY, Song SB et al (2010) Tannic acid and quercetin display a therapeutic effect in atopic dermatitis via suppression of angiogenesis and TARC expression in Nc/Nga mice. *J Invest Dermatol* 130:1459–1463. <https://doi.org/10.1038/JID.2009.401>
- Kaczmarek B (2020) Tannic acid with antiviral and antibacterial activity as a promising component of biomaterials—a mini review. *Materials (Basel)* 13. <https://doi.org/10.3390/MA13143224>
- Kciuk M, Mujwar S, Rani I et al (2022) Computational bioprospecting guggulsterone against ADP ribose phosphatase of SARS-CoV-2. *Molecules* 27. <https://doi.org/10.3390/MOLECULES27238287>
- Khan MF, Kundu D, Hazra C, Patra S (2019) A strategic approach of enzyme engineering by attribute ranking and enzyme immobilization on zinc oxide nanoparticles to attain thermostability in mesophilic *Bacillus subtilis* lipase for detergent formulation. *Int J Biol Macromol* 136:66–82. <https://doi.org/10.1016/J.IJBIO.MAC.2019.06.042>
- Lee JH, Park JH, Cho HS et al (2013) Anti-biofilm activities of quercetin and tannic acid against *Staphylococcus aureus*. *Biofouling* 29:491–499. <https://doi.org/10.1080/08927014.2013.788692>
- Masters L, Eagon S, Heying M (2020) Evaluation of consensus scoring methods for AutoDock Vina, smina and idock. *J Mol Graph Model* 96:107532. <https://doi.org/10.1016/J.JMGM.2020.107532>
- Minhas GS, Bawdon D, Herman R et al (2018) Structural basis of malodour precursor transport in the human axilla. *Elife* 7. <https://doi.org/10.7554/ELIFE.34995>
- Miyazaki M, Yamashita T, Suzuki Y et al (2006) A major urinary protein of the domestic cat regulates the production of feline, a putative pheromone precursor. *Chem Biol* 13:1071–1079. <https://doi.org/10.1016/j.chembiol.2006.08.013>
- Morris GM, Ruth H, Lindstrom W et al (2009) AutoDock4 and AutoDockTools4: automated docking with selective receptor flexibility. *J Comput Chem* 30:2785–2791. <https://doi.org/10.1002/JCC.21256>
- Mujwar S (2021) Computational repurposing of tamibarotene against triple mutant variant of SARS-CoV-2. *Comput Biol Med* 136:104748. <https://doi.org/10.1016/j.compbiomed.2021.104748>
- Mujwar S, Shah K, Gupta JK, Gour A (2021) Docking based screening of curcumin derivatives: a novel approach in the inhibition of tubercular DHFR. *Int J Comput Biol Drug Des* 14:297–314. <https://doi.org/10.1504/IJCBDD.2021.118830>
- Mujwar S, Sun L, Fidan O (2022) In silico evaluation of food-derived carotenoids against SARS-CoV-2 drug targets: crocin is a promising dietary supplement candidate for COVID-19. *J Food Biochem* 46:e14219. <https://doi.org/10.1111/JFBC.14219>
- Mujwar S, Tripathi A (2022) Repurposing benzobromarone as antifolate to develop novel antifungal therapy for *Candida albicans*. *J Mol Model* 28:1–9. <https://doi.org/10.1007/S00894-022-05185-W/FIGURES/6>
- Natsch A, Emter R (2020) The specific biochemistry of human axilla odour formation viewed in an evolutionary context. *Philos Trans R Soc B*:375. <https://doi.org/10.1098/RSTB.2019.0269>
- Ng YJ, Tham PE, Khoo KS et al (2021) A comprehensive review on the techniques for coconut oil extraction and its application. *Bioprocess Biosyst Eng* 44:1807–1818. <https://doi.org/10.1007/S00449-021-02577-9/TABLES/5>
- Oliveira ECCD, Salvador DS, Holsback V et al (2021) Deodorants and antiperspirants: identification of new strategies and perspectives to prevent and control malodor and sweat of the body. *Int J Dermatol* 60:613–619. <https://doi.org/10.1111/IJD.15418>
- Owen AE, Louis H, Agwamba EC et al (2023) Antihypotensive potency of p-synephrine: spectral analysis, molecular properties and molecular docking investigation. *J Mol Struct* 1273:134233. <https://doi.org/10.1016/J.MOLSTRUC.2022.134233>
- Park HJ, Kim HJ, Kwon HJ et al (2006) UVB-induced interleukin-18 production is downregulated by tannic acids in human HaCaT keratinocytes. *Exp Dermatol* 15:589–595. <https://doi.org/10.1111/J.1600-0625.2006.00449.X>
- Payne DE, Martin NR, Parzych KR et al (2013) Tannic acid inhibits *Staphylococcus aureus* surface colonization in an IsaA-dependent manner. *Infect Immun* 81:496. <https://doi.org/10.1128/IAI.00877-12>
- Perumal PO, Mhlanga P, Somboro AM et al (2019) Cytoproliferative and anti-oxidant effects induced by tannic acid in human embryonic kidney (Hek-293) cells. *Biomol* 9:767. <https://doi.org/10.3390/BIOM9120767>
- Priest D (1999) Tea tree oil in cosmeceuticals: from head to toe. In: Southwell I, Lowe R (eds) *Tea Tree*. Harwood academic publishers, Amsterdam, pp 203–206
- Rogério AP, Kanashiro A, Fontanari C et al (2007) Anti-inflammatory activity of quercetin and isoquercitrin in experimental murine allergic asthma. *Inflamm Res* 56:402–408. <https://doi.org/10.1007/S00011-007-7005-6/METRICS>
- Rudden H, Herman R, Rose M et al (2020) The molecular basis of thioalcohol production in human body odour. *Sci Rep* 10:1–14. <https://doi.org/10.1038/s41598-020-68860-z>
- Shah K, Mujwar S, Krishna G, Gupta JK (2020) Computational design and biological depiction of novel naproxen derivative. *Assay Drug Dev Techn* 18:308–317. <https://doi.org/10.1089/ADT.2020.977>
- Shinu P, Sharma M, Gupta GL et al (2022) Computational design, synthesis, and pharmacological evaluation of naproxen-guaiacol chimera for gastro-sparing anti-inflammatory response by selective COX2 inhibition. *Molecules* 27:6905. <https://doi.org/10.3390/MOLECULES27206905/S1>
- Sung HJ, Khan MF, Kim YH (2019) Recombinant lignin peroxidase-catalyzed decolorization of melanin using in-situ generated H<sub>2</sub>O<sub>2</sub> for application in whitening cosmetics. *Int J Biol Macromol* 136:20–26. <https://doi.org/10.1016/J.IJBIO.MAC.2019.06.026>
- Teerasumran P, Velliou E, Bai S, Cai Q (2023) Deodorants and antiperspirants: new trends in their active agents and testing methods. *Int J Cosmet Sci* 45:426–443. <https://doi.org/10.1111/ICS.12852>
- Troccaz M, Gaïa N, Beccucci S et al (2015) Mapping axillary microbiota responsible for body odours using a culture-independent approach. *Microbiome* 3:1–15. <https://doi.org/10.1186/S40168-014-0064-3/SCHEMES/1>
- Troccaz M, Starckenmann C, Niclass Y et al (2004) 3-Methyl-3-sulfanylhexan-1-ol as a major descriptor for the human axilla-sweat odour profile. *Chem Biodivers* 1:1022–1035. <https://doi.org/10.1002/CBDV.200490077>
- Wang X, Wang X, Xia S et al (2023) Effects of tannic acid interfacial absorption on the physicochemical stability of algal oil-loaded

- emulsions and inhibition of fishy off-flavor. *Food Chem* 403:134381. <https://doi.org/10.1016/J.FOODCHEM.2022.134381>
- Watal G, Dhar P, Srivastava SK (2014) Sharma B (2014) Herbal medicine as an alternative medicine for treating diabetes: the global burden. *Evidence-Based Complement Altern Med*. <https://doi.org/10.1155/2014/596071>
- Youness RA, Kamel R, Elkasabgy NA et al (2021) Recent advances in tannic acid (Gallotannin) anticancer activities and drug delivery systems for efficacy improvement: a comprehensive review. *Molecules* 26:–1486. <https://doi.org/10.3390/MOLECULES26051486>
- Zeng XN, Leyden JJ, Spielman AI, Preti G (1996) Analysis of characteristic human female axillary odors: qualitative comparison to

males. *J Chem Ecol* 22:237–257. <https://doi.org/10.1007/BF02055096/METRICS>

**Publisher's note** Springer Nature remains neutral with regard to jurisdictional claims in published maps and institutional affiliations.

Springer Nature or its licensor (e.g. a society or other partner) holds exclusive rights to this article under a publishing agreement with the author(s) or other rightsholder(s); author self-archiving of the accepted manuscript version of this article is solely governed by the terms of such publishing agreement and applicable law.

GCRIIS